AMERICAN SCIENTIFIC PUBLISHERS

Journal of Medical Imaging and Health Informatics
Vol. 4, 416–421, 2014

Evaluation of Four Similarity Measures for 2D/3D Registration in Image-Guided Intervention

Lei Wang[1,2,3], Xin Gao[1,*], Zhiyong Zhou[1], and Xiaocong Wang[4,*]

[1]*Suzhou Institute of Biomedical Engineering and Technology, Chinese Academy of Sciences, Suzhou, 215163, China*
[2]*Changchun Institute of Optics, Fine Mechanics and Physics, Chinese Academy of Sciences, Changchun, 130033, China*
[3]*University of Chinese Academy of Sciences, Beijing, 100049, China*
[4]*1st Hospital of Jilin University, Changchun, 130021, China*

2D/3D medical image registration in image-guided intervention is crucial to assist the clinician to establish the space corresponding relationship between image information and patients' anatomy, which can be quantified by a similarity measure. Among similarity measures, mutual information and its derivatives, were used widely for image registration, and showed significantly differences in the performances of registrations. However, the comparison of their registration performances has not been studied quantitatively yet. Therefore, in this paper, four similarity measures were evaluated for 2D/3D rigid registrations, which are mutual information (MI) and its three derivatives (distance coefficient mutual information (DCMI), distance weighted mutual information (DWMI), gradient weighted mutual information (GWMI)). They were applied to implement registrations based on porcine skull phantom datasets from the Medical University of Vienna, and were evaluated through the mean target registration errors (mTRE) for the registrations. The results demonstrated that the performance of DCMI was the most accurate and robust, and MI was the least effective of the four similarity measures. Moreover, due to the presence of a great amount of soft tissues, GWMI also had the low performance with its mean of mTRE even greater than that by MI, which suggested that intensity gradients were not always having a positive impact for 2D/3D rigid registration when involving a great amount of soft tissues. Between DCMI and DWMI, there were a significant difference in terms of accuracy and robustness, despite using the same image information for them, which means that the construction of an ideal measure should consider not only the image information to be involved but also the construction way of these information.

Keywords: 2D/3D Rigid Registration, Similarity Measure, Mutual Information, Space Distance, Image-Guided Intervention.

1. INTRODUCTION

During Image-guided intervention (IGI),[1] it is crucial to establish the relationship between the space information of image datasets and patient's anatomy. However, the corresponding relationship between the patient's anatomy and the pre-operative image information,[1] in the past, was established subjectively and mentally by the clinician, which leads to poor results during the intervention. In order to avoid the great error of subjective assessment,[2] the traditional method was progressively replaced by 2D/3D image registration technology. During the registration, pre-operative medical images, which are usually three dimensions (3D) CT or MRI, are aligned to two dimension (2D) intra-operative images (X-ray fluoroscopy or Ultrasound) by a space transformation in order to correctly locate the pathological targets.

The goal of 2D/3D rigid registration is to find the space transform, which is applied to pre-operative 3D volume data for combining high-resolution 3D images with real-time 2D images. In the past few years, a variety of 2D/3D rigid registration methods[3–7] were proposed for different intervention operations, which in general can be roughly classified into feature based and intensity based methods.[8]

Feature based methods[9,10] only make use of landmarks (fiducial or natural) or other anatomical features to match images. This makes the type of methods rapidly implemented for 2D/3D rigid registration. Their results can be acted as the gold standard registration when using fixed implants as markers. However, automatic extraction of corresponding features itself is not a trivial procedure. Manual segmentation of features is time-consuming and subjective as well. Because of these disadvantages, this kind of methods has been gradually replaced by intensity based methods[1] and was subjected to less and less studies in 2D/3D rigid registration.

*Authors to whom correspondence should be addressed.

 2156-7018/2014/4/416/006 doi:10.1166/jmihi.2014.1274

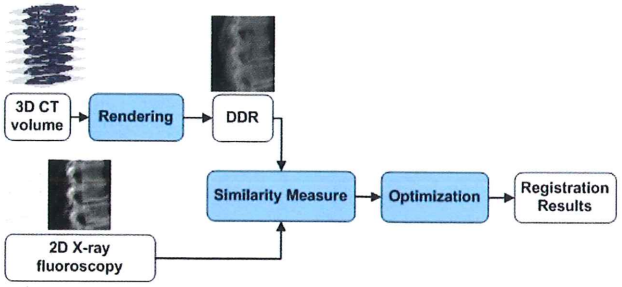

Fig. 1. General process of 2D/3D registration based on intensity methods in image-guided intervention.

Intensity based methods register the images using not the extracted corresponding features but lots of image intensity information.[11] This makes this type of methods generally outperform the feature based methods in terms of accuracy and robustness. However, the images to be registered have different spatial dimensions. Pre-operative volume images usually were rendered and projected to create 2D virtual projection images, called digitally reconstructed radiographs (DRRs) which were compared iteratively with intra-operative 2D image by one selected similarity measure. Having the measure between DRR and intra-operative image, the optimal registration can be achieved by optimization. The process of the registration using intensity based methods is given by Figure 1, in which volume rendering, similarity measure, and optimization are three critical steps for the performance of registration.

A variety of similarity measures have been proposed[3] and were used to construct cost functions for the optimization process of registration. Among the whole of similarity measures, MI nowadays enjoys the great reputation of an accurate and robust multimodality image registration measure[12] which was first proposed in 1995 by Collignon et al.[13] and Viola and Wells[14] as a measure for image registration and further developed in their later papers.[15,16] Since then, it has become a well-known and commonly used similarity measure in medical image registration due to no assumptions and no limits. However, MI cannot work under some conditions, especially for the weak statistical relationship between intensities of images to be registered. This resulted in the propositions of its many derivatives[7,10,12,17–19] by adding extra constrained conditions to original MI, such as space coordinates and image gradients.[10,17] Although these derivatives based on MI had significantly improved performances in registration, they have not yet been quantitatively studied among each other. Therefore, in this paper we take the X-ray fluoroscopy and CT dataset of a porcine skull phantom from the Medical University of Vienna[20] as an example and evaluate the performances of four similarity measures in 2D/3D rigid registrations, i.e., MI and its three modified methods, based on the mean target registration errors (mTRE).[21]

2. METHODS

A variety of registration studies[18,22] show that MI and its derivatives are accurate and robust. We will present four similarity measures in turn: MI and its three derivatives-distance coefficient mutual information (DCMI), distance weighted mutual information (DWMI), gradient weighted mutual information (GWMI).

2.1. Mutual Information

The original mutual information[13] can be given by:

$$MI = \sum_{x,y} p(x,y) \log\left(\frac{p(x,y)}{p(x)p(y)}\right) \quad (1)$$

Where $p(x)$, $p(y)$ are the probability distributions in individual images; $p(x,y)$ is the joint probability distribution and x, y are respectively the intensities of two images. MI need no assumption of a linear relationship between the pixel values of the two images, but instead assumes that the co-occurrence of the most probable values in the two images is maximized at registration.[3]

2.2. Distance Coefficient Mutual Information

MI cannot work well when only the intensities are considered, and space information is not used.[9,10] Therefore, adding extra space information as a constraint (e.g., space coordinates) to MI can overcome the problem to a certain degree. The coordinate of the pixel is one of the key spatial features because it is used to calculate the Euclidean distance to the image origin. Besides, under the conditions of the well-calibrated projection geometry, successful registration means that the two images from the same tissue should have the same intensities and space positions of corresponding pixels theoretically in the same X-ray imaging plate, ignoring differences in image system and formation.[17] Therefore, if the two images were not aligned perfectly, the coordinates of the pixels with the same intensity of two images are not same (Fig. 2). In other words, the distances from the pixels to their respective origins of images are not same. Therefore, the distance difference between pixels with the same intensity in two images can reflect how much two images are aligned with each other.

For example, two kinds of circles (filled and unfilled) in the center of pixels were used to represent two different values of pixels in Figure 2. The distances from the pixels (filled circles) to their respective origins of images can be measured by $fi(i = 1,2,3,4)$ in the floating image, and ri in the reference image, and the distance difference d can be written as:

$$d = (f1+f2+f3+f4) - (r1+r2+r3+r4) \quad (2)$$

Based on the idea mentioned above, a novel similarity measure has been proposed[17] by introducing distance difference to MI, named DCMI in this paper, and expressed as follows:

$$DCMI = \sum_{x,y} \frac{p(x,y)}{1+d(x)^2 d(y)^2} \log\left(\frac{p(x,y)}{p(x)p(y)}\right) \quad (3)$$

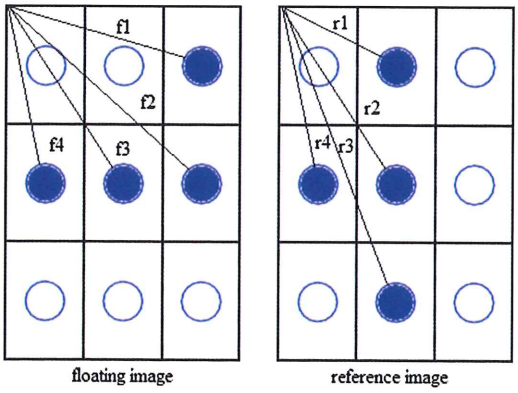

Fig. 2. Respectively Euclidean distances to their own image origins with the same intensity (filled circles).

$$d(x) = \left\| \sum \sqrt{(RI_x^2 + RJ_x^2)} - \sum \sqrt{(FI_x^2 + FJ_x^2)} \right\| \quad (4)$$

Where RI_x, RJ_x and FI_x, FJ_x are the space coordinates of pixel with the same intensity x along the I and J axis in reference and floating image, respectively; $d(x)$ is the Euclidean distance difference between the reference image (X-ray image) and the floating image (DRR image). The greater the distance difference $d(x)$ is, the smaller the probability of co-occurrence is, and smaller DCMI is. When DCMI reached the maximum, two images were considered to be aligned successfully.

2.3. Distance Weighted Mutual Information

Both image intensities and space coordinates are able to measure alignment of two images. There is also another form of combination between them, i.e., weighted sum, which is called DWMI in this paper. The novel similarity measure can be expressed as:

$$DWMI = \sum_{x,y} \left[p(x,y) \log \left(\frac{p(x,y)}{p(x)p(y)} \right) + \frac{\alpha}{(1+d(x)^2)(1+d(y)^2)} \right] \quad (5)$$

Where α is the weighted factor, other parameters are the same as Eq. (4).

2.4. Gradient Weighted Mutual Information

Apart from coordinate information, space information can be also expressed by gradient information, which is pointed in the direction of the greatest rate of increase of image intensity. Introducing it to MI can also improve the performance of MI in registration. Various similarity measures based on intensity gradients of images were proposed. Yim et al.[10] used the weighted sum of mutual information and gradient information, calculated the mutual information in the gradient images (e.g., GI) as well as original images and named GWMI, as similarity measure. GWMI can be given by:

$$GWMI = \beta \cdot MI + \gamma \cdot GI \quad (6)$$

Where GI denote mutual information calculated from the gradient images, β, γ are the weight factors, which decided the contribution to the similarity measure of the intensity and gradient information.

3. EXPERIMENTS AND RESULTS

3.1. Experimental Materials

We compared the four similarity measures by using the 2D X-ray images taken from the anterior-posterior (AP) and lateral (LAT) views as in Figure 3, and 3D CT dataset of the porcine skull phantom, in which the rigid transformation has been already acquired with markers and known as the gold standard.[20] The X-ray images were obtained with an Elekta Synergy linear accelerator, which is equipped with electronic portal imaging device using a PerkinElmer XRD amorphous silicon detector with an active surface of 410×410 mm^2 and a size of 1024×1024 pixels. The 3D CT images were obtained by a 64-slice CT scanner (Philips Brilliance 64, Philips AG, Best, The Netherlands) at 120 kVp and 156 mAs with the spacing of $0.4 \times 0.4 \times 0.8$ mm^3

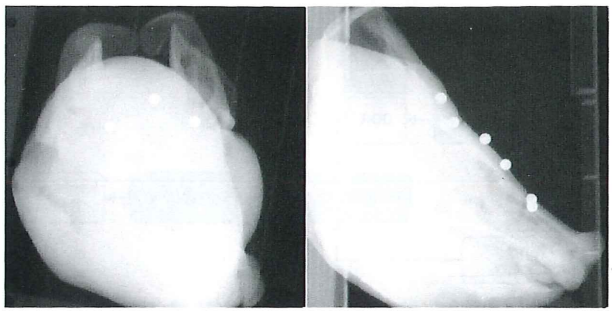

Fig. 3. The left and right images respectively correspond to the X-rays from AP and LAT view.

and the size of $512 \times 512 \times 825$ voxels. More details can be found about the publicly available gold standard data sets in papers.[23]

The implementation of registrations required the intensities of the image to be scaled to 0–255. The X-ray images and the CT volume were isotropically resampled to 1 mm.[24] Moreover, to reduce the influence of a great amount of soft tissues, X-ray images needed to be windowed and CT was used to render and create the DRR image when its intensities greater than a specified threshold value. 70 is selected as the threshold in this paper. To reduce the registration time, the registration is performed in the region of interest (ROI) with a diameter of 200 pixels on the X-ray images with removing the fixed markers as in Figure 4.

After necessarily preprocessing these images, the experiments were begun with setting different starting positions for the optimization in the registration. The starting positions were obtained by distorting the gold standard parameters with a random displacement. The range of displacements was chosen to be $\pm 5°$ and ± 10 mm. These displacements should also reflect the typical range of motion encountered in radiotherapy, for instance, in lung irradiation.[25,26] Then 120 different starting positions were used to evaluate the accuracy and robustness of these measures, which resulted in 120 registrations for each of similarity measures. The accuracy of registration results was quantified based on the mean Target Registration Errors (mTRE). 350 points were spread evenly over the CT and were used as targets for the calculation of mTRE, which can be given by:

$$mTRE = \frac{1}{K} \sum_{i=1}^{K} \| T_{reg} P_i - T_{gold} P_i \| \quad (7)$$

Where P_i is the ith target point; K is the number of target points. T_{gold} denotes the gold standard transformation matrix and T_{reg}

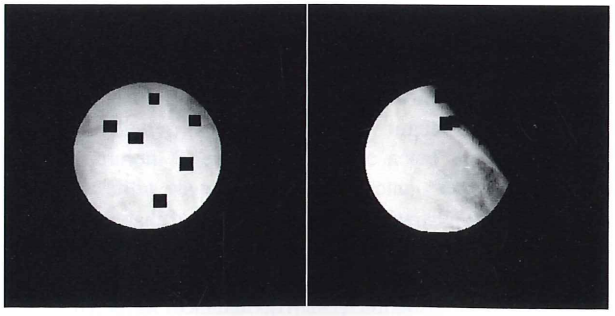

Fig. 4. The left and right images respectively correspond to the ROI of AP and LAT.

Table I. The mean and standard deviations of mTRE and iteration times, as well as the success rate by different measures for the AP.

		mTRE		IterN		
Factor	Measure	Mean	SD	Mean	SD	SR
	MI	11.6630	8.9961	110.1667	22.0146	18/120
(0,1)	GWMI	2.3209	1.9220	78.3417	14.3828	66/120
(1,1)	GWMI	5.4573	6.8542	88.3167	19.0863	52/120
	DCMI	1.6492	0.6902	37.1417	12.9377	87/120
1	DWMI	4.9669	3.5425	111.0833	25.8052	23/120
0.75	DWMI	4.3626	2.6765	104.6750	28.1172	25/120
0.5	DWMI	4.8079	3.3436	108.2417	27.1244	27/120
0.25	DWMI	4.5294	2.8759	107.7833	28.3407	22/120

is the transformation determined by the registration algorithm. The Ray Casting method[27] was used to create DRR of CT dataset without optimization techniques for them, and the Downhill Simplex algorithm[28] was chosen for the optimization. Weight factors α respectively were set to 0.25, 0.5, 0.75 and 1 in Eq. (5). For GWMI in Eq. (6), β, γ were respectively set to 0, 1 resulting in GI, and 1, 1 in this paper.

3.2. Results

Since the registrations were implemented repeatedly 120 times for each measure, it is necessary to use the 120 times registration results to evaluate the registration performance of each measure. The final accuracy of these measures was given as the mean and standard deviation (SD) of mTRE and iteration times, (e.g., IterN) after the registration, as well as the success rate (SR), defined as the portion of successful against all registrations and successful threshold was set to 2 mm.

The registration results in Tables I and II for AP and LAT respectively showed that the mean of mTRE by DCMI was lower by at least 28.94% and at most 88.14% than those by the other measures, with the highest success rate, i.e., 72.50% for AP and 74.17% for LAT, which were showed in Figure 6 for AP and LAT X-rays. The standard deviations of mTRE by DCMI also were the smallest than those by MI, GWMI and DWMI. It reduced from 8.9961 mm and 5.2832 mm by MI to 0.6902 mm and 5.2832 mm by DCMI for AP and LAT, respectively. The significant decrease of standard deviations of mTRE suggested that DCMI was more accurate and robust for 2D/3D rigid registration than those of the other measures. Meanwhile, the results also showed that the registrations using DCMI took less time than those of MI, GWMI and DWMI, with the mean of iteration times smaller by at least 52.59% and at most 66.56% than those by the others. Hence, it is likely to use DCMI for the real-time image guided intervention

Table II. The mean and standard deviations of mTRE and iteration times, as well as the success rate by different measures for the LAT.

		mTRE		IterN		
Factor	Measure	Mean	SD	Mean	SD	SR
	MI	12.2653	5.2832	115.6250	20.2265	0/120
(0,1)	GWMI	13.1988	5.1752	97.5833	12.6528	0/120
(1,1)	GWMI	11.0411	4.1631	99.6667	13.9274	0/120
	DCMI	1.5657	0.6846	64.1833	7.9388	89/120
1	DWMI	4.7306	5.0473	99.5750	19.7704	47/120
0.75	DWMI	6.3563	6.2150	103.7750	19.2949	32/120
0.5	DWMI	6.2521	5.8528	105.1417	22.1114	31/120
0.25	DWMI	6.3344	6.0388	105.6667	22.8496	35/120

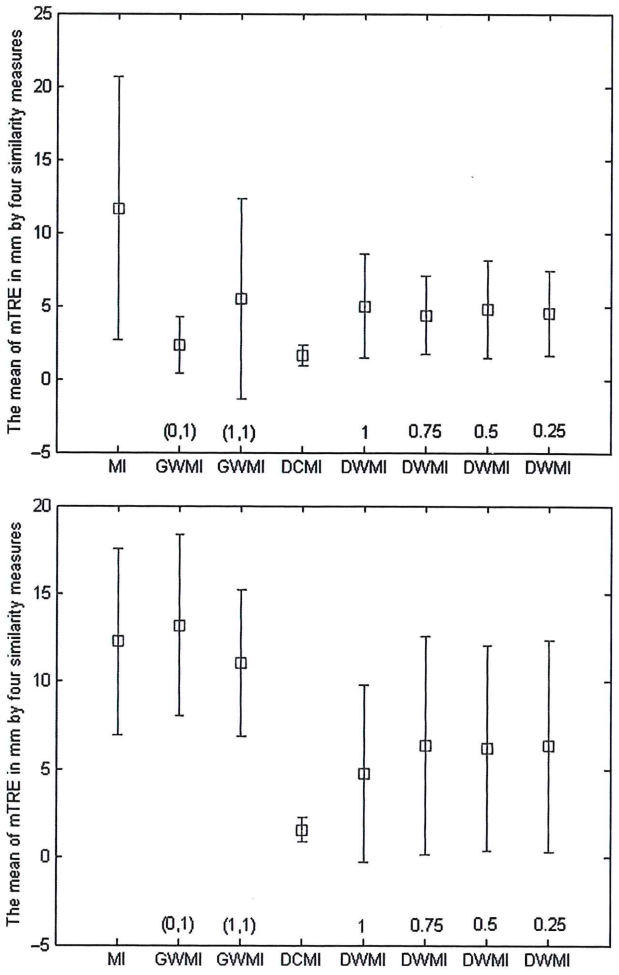

Fig. 5. The top and bottom correspond to the mean and standard deviations of mTRE by different measures for AP and LAT.

systems. From the statistical analysis above, the conclusion can be reached that DCMI was the best performance of registration in terms of accuracy and robustness.

For DWMI and DCMI, they were constructed by the same image information, i.e., image intensities and space distances from the pixel coordinates, but their performances of registration were significantly different, with both better than those by MI. This means that when using the same image information, the way of constructing similarity measures had a significant influence on the registration performances of measures. For DWMI, the weighted factor of it had an influence to the registration performance as in Figures 5 and 6. However, their influence cannot be objectively estimated due to the existence of a great amount of soft tissues, which led DWMI not to be stable for the registrations in this paper. For example, among of different weights for DWMI, the registrations by DWMI obtained the highest success rate for AP but the lowest success rate for LAT when weight α was set to 0.5.

Similar to DWMI, both MI and GWMI also were not stable for registrations in this paper showed in Figure 6. The mean of mTRE by MI were greater by at least 0.9296 times and at most 6.8337 times than those of DCMI and DWMI, with no successful registration for LAT. The performance of GWMI varied greatly with the weighted factors β, γ. When β and γ were respectively

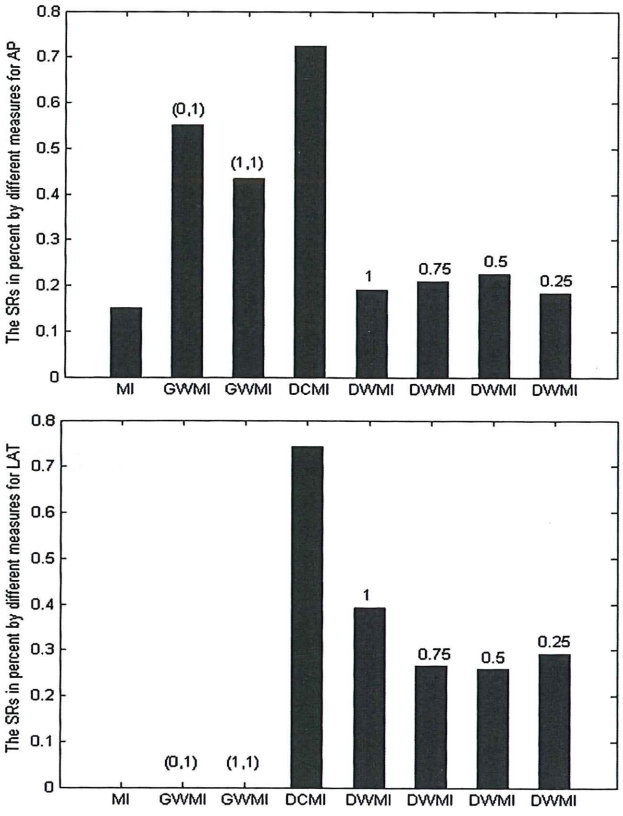

Fig. 6. The top and bottom correspond to the success rates by different measures for AP and LAT.

set to 0 and 1, GWMI can work well relative to MI, and its mean of mTRE was lower by 4.0252 times for AP but greater by 0.7073 times for LAT. Under the same conditions, its success rates were respectively 55.00% and 0%. The great differences of the results for AP and LAT suggested that intensity gradients were not always having a positive impact to similarity measure for 2D/3D rigid registration, especially when images to be registered involving lots of soft tissues. According to the analysis, we can conclude that thought MI and its variants were famous for multimodality image registration measures; they cannot work well for 2D/3D rigid registration in some cases.

4. CONCLUSIONS

In this paper, we used X-ray fluoroscopy and CT dataset of a porcine skull phantom from the Medical University of Vienna to evaluate four similarity measures (MI, DCMI, DWMI, GWMI) for 2D/3D rigid registration through the mean and standard deviation of mTRE and iteration times after the registrations, as well as the success rate. The experiment results showed that DCMI was more accurate and robust than the other measures. By adding the space distance information to MI, both DCMI and DWMI could improve registration efficiency and avoid the limitations of similarity measures constructed with the single image information (e.g., intensity and/or its gradient information) in 2D/3D rigid registration, and achieve the registration with different SRs for AP and LAT. Though DCMI and DWMI have the better performances of registration, they were significantly different for 2D/3D registration in terms of accuracy and robustness. This indicates that the way of construction of them has a great influence on the performance of registration although they used the same information of the space distances and image intensities for similarity measures. Meanwhile, the results also showed that due to the presence of lots of soft tissues, MI and GWMI were instable for rigid registration with low SR for AP but no SR for LAT, which meant that intensity gradients were not always having an important improvement for registration performance by integrating them with similarity measures. Therefore, the construction of an ideal similarity measure should consider not only the information to be involved but also the way of the construction of this information.

Acknowledgments: We sincerely thank Professor W. Birkfellner for his gold standard datasets and the corresponding code for DRR. We also thank C. Andreas, a student of Birkfellner, who gave me great assistance about how to use their datasets. This work was supported by National Natural Science Foundation of China (81000651, 81371640), Science and Technology Plan Project of Suzhou (SH201210), Special Project in Clinical Medicine of Jiangsu Province, China (BL2012049), Science and Technology Plan Project of Jiangsu Province, China (BK2012188).

References and Notes

1. P. Markelj, D. Tomazevic, B. Likar, and F. Pernus, A review of 3D/2D registration methods for image-guided interventions. *Med. Image Anal.* 16, 642 **(2012)**.
2. P. Markelj, D. Tomazevic, F. Pernus, and B. Likar, Robust gradient-based 3-D/2-D registration of CT and MR to X-ray images. *Med. Imaging, IEEE Transactions on* 27, 1704 **(2008)**.
3. G. P. Penney, J. Weese, J. A. Little, P. Desmedt, and D. L. G. Hill, A comparison of similarity measures for use in 2-D-3-D medical image registration. *Medical Imaging, IEEE Transactions on* 17, 586 **(1998)**.
4. J. H. Hipwell, G. P. Penney, R. A. McLaughlin, K. Rhode, P. Summers, T. C. Cox, J. V. Byrne, J. A. Noble, and D. J. Hawkes, Intensity-based 2-D-3-D registration of cerebral angiograms. *Medical Imaging, IEEE Transactions on* 22, 1417 **(2003)**.
5. J. Kim, L. Shidong, D. Pradhan, R. Hammoud, Q. Chen, F. F. Yin, Y. Zhao, H. O. K. I. M. Jae, and B. Movsas, Comparison of similarity measures for rigid-body CT/dual x-ray image registrations. *Technology in Cancer Research and Treatment* 6, 337 **(2007)**.
6. M. Lu, Acceleration method of 3D medical images registration based on compute unified device architecture. *Bio-Medical Materials and Engineering* 24, 1109 **(2014)**.
7. Y. C. Sun, F. S. Yuan, H. Li, Y. J. Zhao, P. J. Lv, and Y. Wang, Evaluation of the accuracy of a common regional registration method for three-dimensional reconstruction of edentulous jaw relation by a 7-axis three-dimensional measuring system. *Bio-Medical Materials and Engineering* 24, 1275 **(2014)**.
8. D. Xu, S. Xu, D. A. Herzka, R. C. Yung, M. Bergtholdt, L. F. Gutierrez, and E. R. McVeigh, 2D/3D registration for X-ray guided bronchoscopy using distance map classification, *Engineering in Medicine and Biology Society (EMBC), 2010 Annual International Conference of the IEEE* **(2010)**, pp. 3715–3718.
9. J. Pluim, J. Maintz, and M. Viergever, Image registration by maximization of combined mutual information and gradient information. *Medical Imaging, IEEE Transactions on* 19, 809 **(2000)**.
10. Y. Yim, X. Chen, M. Wakid, S. Bielamowicz, and J. Hahn, 2D-3D registration using gradient-based MI for image guided surgery systems, SPIE in Medical Imaging 2011: Visualization, Image-Guided Procedures, and Modeling, edited by K. H. Wong and D. R. Holmes, International Society for Optics and Photonics, Lake Buena Vista, Florida **(2011)**, Vol. 7964.
11. A. Khamene, P. Bloch, W. Wein, M. Svatos, and F. Sauer, Automatic registration of portal images and volumetric CT for patient positioning in radiation therapy. *Med. Image Anal.* 10, 96 **(2006)**.
12. D. Tomazevic, B. Likar, and F. Pernus, 3-D/2-D registration by integrating 2-D information in 3-D. *Medical Imaging, IEEE Transactions on* 25, 17 **(2006)**.
13. A. Collignon, F. Maes, D. Delaere, D. Vandermeulen, P. Suetens, and G. Marchal, Automated multi-modality image registration based on information theory. *Information Processing in Medical Imaging* 3, 263 **(1995)**.
14. P. Viola and W. M. Wells III, Alignment by maximization of mutual information. *International Journal of Computer Vision* 24, 137 **(1997)**.

15. F. Maes, A. Collignon, D. Vandermeulen, G. Marchal, and P. Suetens, Multimodality image registration by maximization of mutual information. *Medical Imaging, IEEE Transactions on* 16, 187 **(1997)**.
16. W. M. Wells, P. Viola, H. Atsumi, S. Nakajima, and R. Kikinis, Multi-modal volume registration by maximization of mutual information. *Med. Image Anal.* 1, 35 **(1996)**.
17. L. Wang, X. Gao, and Q. Fang, A novel mutual information-based similarity measure for 2D/3D registration in image guided intervention, *2013 International Conference on Orange Technologies (ICOT)*, IEEE, Tainan, Taiwan **(2013)**, pp. 135–138.
18. J. P. W. Pluim, J. B. A. Maintz, and M. A. Viergever, Mutual-information-based registration of medical images: A survey. *Medical Imaging, IEEE Transactions on* 22, 986 **(2003)**.
19. S. S. Wang, Y. Xia, P. Dong, J. H. Luo, Q. Huang, D. G. Feng and Y. X. Li, Bias Correction for magnetic resonance images via joint entropy regularization1. *Bio-Medical Materials and Engineering* 24, 1239 **(2014)**.
20. C. Gendrin, P. Markelj, S. A. Pawiro, J. Spoerk, C. Bloch, C. Weber, M. Figl, H. Bergmann, W. Birkfellner, B. Likar, and F. Pernus, Validation for 2D/3D registration II: The comparison of intensity- and gradient-based merit functions using a new gold standard data set. *Medical Physics* 38, 1491 **(2011)**.
21. E. B. van de Kraats, G. P. Penney, D. Tomazevic, T. van Walsum, and W. J. Niessen, Standardized evaluation methodology for 2-D-3-D registration. *Medical Imaging, IEEE Transactions on* 24, 1177 **(2005)**.
22. F. Maes, D. Vandermeulen, and P. *Suetens*, Medical image registration using mutual information. *Proceedings of the IEEE* 91, 1699 **(2003)**.
23. S. Pawiro, P. Markelj, F. Pernus, C. Gendrin, M. Figl, C. Weber, F. Kainberger, I. N. Huhmann, H. Bergmeister, and M. Stock, Validation for 2D/3D registration I: A new gold standard data set. *Medical Physics* 38, 1481 **(2011)**.
24. S. Pawiro, P. Markelj, C. Gendrin, M. Figl, M. Stock, C. Bloch, C. Weber, E. Unger, I. Noebauer, F. Kainberger, H. Bergmeister, D. Georg, H. Bergmann, and W. Birkfellner, A new gold-standard dataset for 2D/3D image registration evaluation, SPIE in Medical Imaging 2010: Visualization, Image-Guided Procedures, and Modeling, edited by K. H. Wong and M. I. Miga, International Society for Optics and Photonics, San Diego, California, USA **(2010)**, Vol. 7625.
25. T. Künzler, J. Grezdo, J. Bogner, W. Birkfellner, and D. Georg, Registration of DRRs and portal images for verification of stereotactic body radiotherapy: A feasibility study in lung cancer treatment. *Physics in Medicine and Biology* 52, 2157 **(2007)**.
26. W. Birkfellner, M. Stock, M. Figl, C. Gendrin, J. Hummel, S. Dong, J. Kettenbach, D. Georg, and H. Bergmann, Stochastic rank correlation: A robust merit function for 2D/3D registration of image data obtained at different energies. *Medical Physics* 36, 3420 **(2009)**.
27. J. Spork, A high-performance GPU based rendering module for distributed, real-time, rigid 2D/3D image registration in radiation oncology, M.Sc. Thesis, College of Information **(2010)**.
28. S. A. Teukolsky, W. T. Vetterling, B. P. Flannery, and H. William, Press. Numerical Recipes in $C++$: The Art of Scientific Computing, Pearson Education **(1992)**.

Received: 8 July 2013. Accepted: 8 December 2013.